*Carcinogenesis*, 2020, Vol. 41, No. 6, 723–733

**doi:10.1093/carcin/bgz180**
Advance Access publication October 30, 2019
Original Article

ORIGINAL ARTICLE

# EGFR-PKM2 signaling promotes the metastatic potential of nasopharyngeal carcinoma through induction of FOSL1 and ANTXR2

Shengnan Chen[1,2,3], Tang Youhong[4], Yixin Tan[5], Yuxiang He[4], Yuanyuan Ban[1,2,3], Jing Cai[1,2,3], Xiaoling Li[1,2,3], Wei Xiong[1,2,3], Zhaoyang Zeng[1,2,3], Guiyuan Li[1,2,3], Mei Yi[2,6], Wei Liu[2,7] and Bo Xiang[1,2,3,*]

[1]Hunan Provincial Cancer Hospital and Cancer Hospital Affiliated to Xiangya Medical School, Central South University, Changsha, Hunan 410013, [2]NHC Key Laboratory of Carcinogenesis (Central South University) and Key Laboratory of Carcinogenesis and Cancer Invasion of the Chinese Ministry of Education, Cancer Research Institute, Central South University, Changsha, Hunan 410078, [3]Hunan Key Laboratory of Nonresolving Inflammation and Cancer, Disease Genome Research Center, The Third Xiangya Hospital, Central South University, Changsha, Hunan, [4]Department of Oncology, Xiangya Hospital, Central South University, Changsha, Hunan, 410008, [5]Department of Dermatology, Second Xiangya Hospital, Central South University, Hunan Key Laboratory of Medical Epigenetics, Changsha, 410011, Hunan, [6]Department of Dermatology, Xiangya Hospital, Central South University, Changsha, Hunan 410008 and [7]Department of Endocrinology, Second Xiangya Hospital, Central South University, Changsha 410011, China

* To whom correspondence should be addressed. Bo Xiang, Tel: +86 731 83867186; Fax: +86 731 84805383; Email: xiangbolin@csu.edu.cn
Correspondence may also be addressed to Wei Liu, Tel: +86 731 85295246; Email: liuwei_13510@163.com

## Abstract

Nasopharyngeal carcinoma (NPC) is notorious for its aggressiveness and high metastatic potential. NPC patients with distant metastasis have a particularly poor prognosis; however, evaluating metastatic potential by expression profiles of primary tumors is challenging. This study aimed to investigate the association between activation of epidermal growth factor receptor (EGFR) signaling and NPC metastasis and the underlying mechanisms. We found an association between EGFR protein overexpression and intense EGFR immunostaining in NPC samples with advanced tumor node metastasis stage, clinical stage, and distant metastasis in NPC patients. Exogenous EGF stimulates NPC mobility and invasiveness *in vitro*. Activation of EGFR signaling prompted PKM2 translocation to the nucleus. Silencing either EGFR or PKM2 attenuates NPC cell aggressiveness *in vitro* and *in vivo*. Blocking EGFR signaling with cetuximab suppressed NPC cell invasiveness *in vitro* and metastatic potential *in vivo*. Comprehensive analyses of transcriptome profiles indicated that the EGFR-PKM2 axis activates a number of novel metastasis promoters, including F3, FOSL1, EPHA2, ANTXR2, and AKR1C2. Finally, we found that the metastasis-promoting function of the EGFR-PKM2 axis is dependent on nuclear PKM2 regulation of the transcription of metastasis-related genes, including FOSL1 and ANTXR2. Our study indicates that EGFR-PKM2 signaling promotes NPC cell invasion and metastasis through induction of FOSL1 and ANTXR2 and identifies EGFR as a promising biomarker for predicting the risk of distant metastasis.

## Introduction

Nasopharyngeal carcinoma (NPC) is a unique subtype of head and neck squamous cell carcinoma (HNSCC) prone to distant metastasis and prevalent in South China and South East Asia (1). NPC exhibits a distinct etiological and geographical distribution and commonly metastasizes to the lungs, liver, and bones. The incidence rate of distant metastatic NPC at presentation

**Received:** 7 May 2019; **Revised:** 13 October 2019; **Accepted:** 24 October 2019

**Abbreviations**

| | |
|---|---|
| AA | arachidonic acid; |
| EGFR | epidermal growth factor receptor; |
| FBS | fetal bovine serum; |
| GSEA | gene set enrichment analysis; |
| NPC | Nasopharyngeal carcinoma; |
| OS | overall survival; |
| PKM2 | pyruvate kinase M2 |

varies from 7.7 to 20.3% (2–6). Although significant improvement in local control has been achieved by the use of high precision radiotherapy, treatment failure for distant metastasis is still the primary cause of death from NPC. Given the high mortality rate of distant metastatic NPC, it is critical to identify novel targets and develop new strategies for antimetastasis therapy (7–10).

The epidermal growth factor receptor (EGFR) is a transmembrane protein in the ErbB family, a subfamily of four closely related receptor tyrosine kinases. Upon binding with its cognate ligand EGF, intracellular EGFR tyrosine phosphorylation and receptor dimerization with other family members lead to enhanced cell proliferation (11). The EGFR protein is frequently overexpressed in a wide variety of human cancers and promotes cell growth and proliferation. Blocking EGFR signaling by antibodies or inhibition of its intracellular tyrosine kinase activity suppresses tumor cell growth and improves patient condition. Genomic sequencing studies have revealed that *EGFR* mutations are rare in NPC samples (12–15). Although its growth promotive role is well established, the contribution of EGFR to NPC metastasis remains elusive. Activation of EGFR signaling promotes the invasiveness of NPC cells (16,17); however, the downstream effectors involved in EGFR signaling-mediated tumor invasion and metastasis have not been identified.

Increased dependence on aerobic glycolysis and overexpression of glycolytic enzymes is an emerging hallmark of cancer; this phenomenon is called the Warburg effect (18,19). Pyruvate kinase M2 (PKM2) is the rate-limiting enzyme catalyzing the formation of pyruvate from the conversion of phosphoenolpyruvate. PKM2 is the fetal isoform of pyruvate kinase but is overexpressed in various human cancers (20). PKM2 localizes to the cell nucleus and regulates gene transcription (21). Activation of EGFR signaling induces nuclear translocation of PKM2 and stimulates cyclin D1 (CCND1) transcription (22). Recent evidence suggests a crucial role for PKM2 in pancreatic cancer metastasis (23). Nevertheless, the role of PKM2 in NPC metastasis remains elusive.

The objective of this study was to investigate the association between EGFR-PKM2 signaling and NPC metastasis and the underlying mechanism of action, in order to identify novel targets for antimetastasis therapy for NPC.

## Materials and methods

### NPC samples and immunohistochemistry

A cohort of clinical samples, including 309 NPC cases and 92 samples of noncancerous inflammatory nasopharyngeal epithelial tissues, was obtained between January 2012 and October 2017 from the Pathology Department of Cancer Hospital affiliated with the Xiangya Medical School, Central South University (Hunan, China). All patients provided signed consent to participate. A polyclonal anti-EGFR antibody was obtained from Maxin, Inc. (Fuzhou, China). EGFR protein was detected by immunohistochemical staining according to methods described previously (8,24). A staining index (values, 0–6) was calculated from the staining intensity (scores: negative = 0, weak = 1, moderate = 2, or strong = 3) and the percentage of stained tumor cells (scores: <10% = 1, 10–50% = 2, >50% = 3). The sum of these two scores was used as the final immunoreactive score (0–6), i.e. low expression (0–2 scores) and high expression (3–6 scores). This study, which involved the use of clinical samples, was approved by the Institute Research Ethics Committee.

### Cell lines and culture

A well-differentiated NPC cell line (HK1) (25) and a hypopharyngeal carcinoma cell line (FaDu) (26,27) were routinely maintained in our laboratory. Cells were grown in RPMI-1640 medium supplemented with 10% fetal bovine serum (FBS) and penicillin/streptomycin (Gibco, Grand Island, NY, USA) in a humidified incubator at 37°C with 5% $CO_2$ and 95% air. The cells were authenticated by short tandem repeat analysis by Life Technologies every 6 months. Cells were treated with recombinant EGF (SinoBiological, Inc., Beijing, China) at 100 ng/ml or micheliolide (MCL, MedChemExpress, Beijing, China) at 5 μM or cetuximab (Erbitux®, Merck KGaA, Darmstadt, Germany) at 20 ng/ml.

### siRNA, shRNA, and gene transfection

All gene targeting siRNAs and scrambled siRNAs used in this study were purchased from GenePharma (Shanghai, China). By using Lipofectamine® RNAiMAX Reagent (Invitrogen, Carlsbad, CA, USA), siRNAs were transfected into NPC cells according to the manufacturer's protocol. The siRNA sequences are listed in Supplementary Table S1, available at *Carcinogenesis* Online.

### RNA isolation and real-time reverse transcription PCR (RT-qPCR)

TRIzol Reagent (Invitrogen, San Diego, CA, USA) was used to extract total RNA as previously described (28). Residual genomic DNA in total RNA samples was removed by RNase-free DNase I (Roche Diagnostics, Rotkreuz, Switzerland), and 1 μg of total RNA was reverse transcribed to cDNA using M-MLV reverse transcriptase (Invitrogen, San Diego, CA, USA). The mRNA levels were evaluated by the CFX96 Touch™ Real-Time PCR Detection System (Bio-Rad, Hercules, CA, USA) using SYBR Green I (Selleck, Shanghai, China). The primer sequences are listed in Supplementary Table S2, available at *Carcinogenesis* Online.

### Immunofluorescence and fluorescence-activated cell sorting (FACS) assays

For the immunofluorescence assay, tumor cell suspensions were fixed with 4% paraformaldehyde. After fixation, cetuximab or human IgG was incubated with tumor cells for 24 h at 4°C, and then the cells were stained by FITC-conjugated secondary antibody. The frequency of antibody-labeled tumor cells was measured by flow cytometry (BD Biosciences, San Jose, CA, USA).

### RNA-seq

Total RNA was isolated using the TRIzol reagent (Invitrogen). A Bioanalyzer 2100 (Agilent Technologies, Palo Alto, CA, USA) was used to monitor the integrity of the RNA samples. RNA-seq was performed with the Illumina-PE150 sequencer (Illumina Inc., San Diego, CA, USA). The NOISeq method was employed to identify differentially expressed genes with a 1.5-fold change between two groups (29). Gene set enrichment analysis (GSEA) was performed as described previously (30).

### Chromatin immunoprecipitation (ChIP) and qPCR

For ChIP analysis, cells grown on a 10-cm plate were processed as described in the ChIP Assay kit (17-295) protocol (Millipore, Billerica, MA, USA). The PKM2-associated chromatin was immunoprecipitated by an anti-PKM2 antibody (Cell Signaling Technology; Cat No. 8685S). The precipitated DNA fragments were purified and measured by qPCR under the conditions described above. Primers specific to each segment of interest are listed in Supplementary Table S3, available at *Carcinogenesis* Online.

### Protein extraction and western blotting

Cellular proteins were extracted using a lysis buffer (Beyotime, Jiangsu, China), separated by SDS-PAGE, and then transferred onto PVDF membranes (Millipore). Protein levels were detected with the following

antibodies: polyclonal anti-EGFR (Proteintech; Cat No. 18986-1-AP), polyclonal anti-PKM2 (Cell Signaling Technology; Cat No. 4053T), anti-FOSL1 (Abclonal; Cat No. A5372), anti-ANTXR2 (Abclonal; Cat No. A6526), anti-histone H3 (Cell Signaling Technology; Cat No. 4499), and anti-GAPDH (BBI Life Sciences; Cat No. D190090-0100).

## Cell migration and invasion assays

Tumor cell mobility or invasiveness was evaluated using 8-μm-pore Transwell inserts (Corning-Costar, Cambridge, MA, USA) precoated with or without 15 μl of Matrigel (BD Biosciences, Bedford, MA, USA), respectively. Briefly, single-cell suspensions in serum-free RPMI-1640 medium (Gibco) were plated onto the upper inserts at a density of 100 000 cells/well and then the inserts were placed into the lower chamber with 600 μl of culture medium containing 15% FBS. Cells in the Transwell inserts were incubated for 6–24 h at 37°C to allow cells to migrate or invade across the membrane. Cells that had migrated or invaded were then visualized with crystal violet dye. The average number of migrated or invaded cells from five random fields was counted.

## *In vivo* tumor metastasis and *in vivo* bioluminescent assays

All animal experiments were performed according to the guidelines of the Ethical Review Committee of Central South University of China. HK1 cells were infected with a luciferase-expressing lentivirus. Single-tumor cell suspensions ($1 \times 10^6$/0.2 ml) in serum-free RPMI-1640 were orthotopically transplanted into the livers of 6-week-old male BALB/c nude mice (31,32)

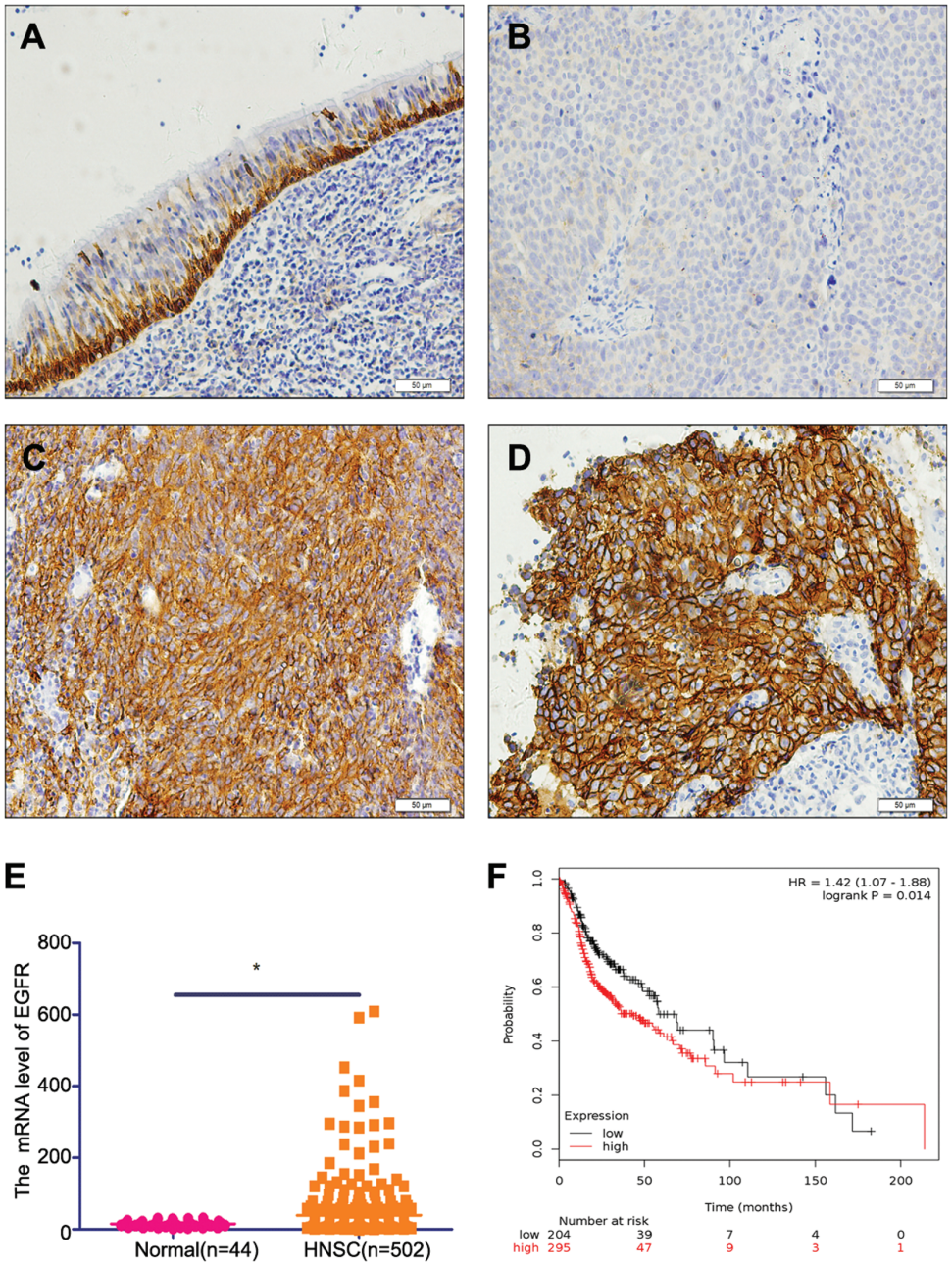


**Figure 1.** High expression of EGFR is associated with distant metastasis in NPC **(A)** Immunostaining of EGFR protein is restricted in the basal layer of normal nasopharyngeal epithelium, but not in the differentiated columnar epithelial cells. **(B)** Negative staining of EGFR in a subset of NPC samples. **(C)** Moderate immunostaining of EGFR protein in NPC samples without distant metastasis. **(D)** Intense immunostaining of EGFR protein in NPC samples with distant metastasis. **(E)** mRNA levels of EGFR are elevated in head and neck cancer. **(F)** High expression of EGFR predicts unfavorable clinical outcomes in head and neck cancer patients. *$p < 0.05$).

(Shanghai SLAC Laboratory Animal Co. Ltd., Shanghai, China). Two weeks posttransplantation, the mice were intraperitoneally injected with cetuximab (Merck Millipore, Darmstadt, Germany) at a dose of 5 mg/kg. hIgG (5 mg/kg) was used as a negative control. The average body weight for each group was determined weekly. After 8 weeks of treatment, the mice were intraperitoneally injected with a luciferin solution at a dose of 150 mg/kg (15 mg/ml in PBS). Metastatic tumors were evaluated once by the *in vivo* bioluminescent assay at 8 weeks posttransplantation, after which the mice were sacrificed (31); the liver tissues were obtained, fixed in 4% saline-buffered formalin, embedded in paraffin, sectioned at 5 μm and stained with hematoxylin and eosin (H&E).

### Statistical analysis

Differences in the quantitative variables between groups were analyzed by Student's *t* test. The Pearson's Chi-square test was used to analyze the association of EGFR expression with clinicopathological characteristics using the SPSS 13.0 software package (SPSS, Chicago, IL, USA). A value of $P < 0.05$ was considered statistically significant.

## Results

### Overexpression of EGFR in NPC is associated with advanced clinical stage and distant metastasis

The levels of EGFR protein in NPC samples were evaluated by immunohistochemical staining. As shown in Figure 1A, immunostaining of EGFR protein is restricted in the basal cells in noncancerous nasopharyngeal epithelium, but not in the differentiated pseudostratified multiciliated columnar epithelial cells. Only 17 out of 309 NPC samples (5.5%) exhibited negative staining for EGFR protein (Figure 1B). Moderate (Figure 1C) to high levels (Figure 1D) of membrane staining for EGFR protein are observed in the majority of NPC samples (292 out of 309, 94.5%). Among the EGFR-positive NPC samples, 90 out of 309 (30.42%) exhibit intense membrane staining for EGFR protein. The association of EGFR expression with clinicopathological features was analyzed (Table 1). EGFR expression was not associated with gender, but intense EGFR staining was associated with patient age, advanced tumor node metastasis stage, clinical stage, and distant metastasis status. We also analyzed the association of expression levels of EGFR mRNA with overall survival (OS) in HNSCC. According to The Cancer Genome Atlas (TCGA) dataset, high expression of EGFR mRNA predicts a worse prognosis than low expression of EGFR mRNA ($P < 0.01$, Figure 1E and F).

### Activation of EGFR signaling promotes migration and invasiveness of NPC *in vitro*

The association of EGFR levels with distant metastasis prompted us to ask whether overexpression of EGFR contributes to higher mobility and invasiveness in NPC. As shown in Figure 2A and B, recombinant EGF treatment stimulates migration and invasiveness of HK1 and FaDu cells. Transient transfection of two separate siRNAs targeting EGFR successfully inhibits the expression of EGFR in HK1 and FaDu cells at both the mRNA and protein level (Figure 2C). As a result, transient silencing of EGFR expression by two siRNAs markedly inhibits the migration and invasiveness of HK1 and FaDu cells (Figure 2D and E). When EGFR mRNA and protein levels in HK1 and FaDu cells were stably knocked down by shRNA-expressing lentivirus (Figure 2F), the migration and invasion of NPC cells were markedly inhibited (Figure 2G and H).

### Blockage of EGFR signaling by cetuximab inhibits metastasis *in vivo*

We then investigated the effects of blocking EGFR signaling by the EGFR monoclonal antibody cetuximab on NPC cell migration and invasion and found that cetuximab prevents invasiveness *in vitro* (Figure 3A and B). We also measured the binding of cetuximab on the tumor cell surface by FACS assays. The results showed that more than 99% of HK1 cells, compared to 76.5% of FaDu cells, bind cetuximab (Supplementary Figure S1, available at *Carcinogenesis* Online), which is in consistent with the results showing that HK1 cells are more sensitive to cetuximab-mediated suppression of migration and invasiveness than FaDu cells (Figure 3A and B). Hepatic subcapsular transplantation was employed to evaluate whether blockage of EGFR signaling by cetuximab inhibits NPC cells metastasis *in vivo*. HK1 cells infected with a luciferase-expressing lentivirus were transplanted into the livers of nude mice. Two weeks after transplantation, cetuximab was intraperitoneally injected at 1 mg/kg weekly. hIgG was used as a negative control. During the cetuximab treatment period, we observed no difference in the weight of the mice between groups (Figure 3C). After 8 weeks of treatment, hepatic metastasis evaluated by an *in vivo* bioluminescent assay revealed that cetuximab treatment effectively suppressed HK1 cell metastasis of the livers of nude mice (Figure 3D). Morphological analysis (Figure 3E) and H&E staining (Figure 3F) confirmed that there were fewer metastatic tumor loci in the livers of cetuximab-treated mice than in the hIgG-treated control group.

### Nuclear PKM2 contributes to EGFR signaling-mediated NPC cell migration and invasion

It has been demonstrated that PKM2 translocates to the nucleus and functions as a transcription cofactor upon activation of EGFR signaling (22,33). To study the role of PKM2 in NPC cell

**Table 1.** High expression of EGFR protein is associated with advanced NPC progression and distant metastasis.

| | | | Expression of EGFR | | Pearson's Chi-square test | | |
|---|---|---|---|---|---|---|---|
| Factor | Class | Sample No. | Low (0–4) | High (5,6) | $\chi^2$ | df | *P* |
| Gender | Male | 228 | 156 (68.4%) | 72 (31.6%) | 0.5513 | 1 | 0.4578 |
| | Female | 81 | 59 (72.8%) | 22 (27.2%) | | | |
| Age | < 50 | 83 | 65 (78.3%) | 18 (21.7%) | 4.09 | 1 | 0.043 |
| | ≥50 | 226 | 150 (66.4%) | 76 (33.6%) | | | |
| TNM | T1-T2 | 138 | 106 (76.8%) | 32 (23.2%) | 6.162 | 1 | 0.013 |
| | T3-T4 | 171 | 109 (63.7%) | 62 (36.3%) | | | |
| Clinical stage | I–III | 171 | 129 (75.4%) | 42 (24.6%) | 6.210 | 1 | 0.0127 |
| | IV | 138 | 86 (62.3%) | 52 (37.7%) | | | |
| Metastasis | No | 257 | 187 (72.8%) | 70 (27.2%) | 7.312 | 1 | 0.0069 |
| | Yes | 52 | 28 (53.9%) | 24 (46.1%) | | | |

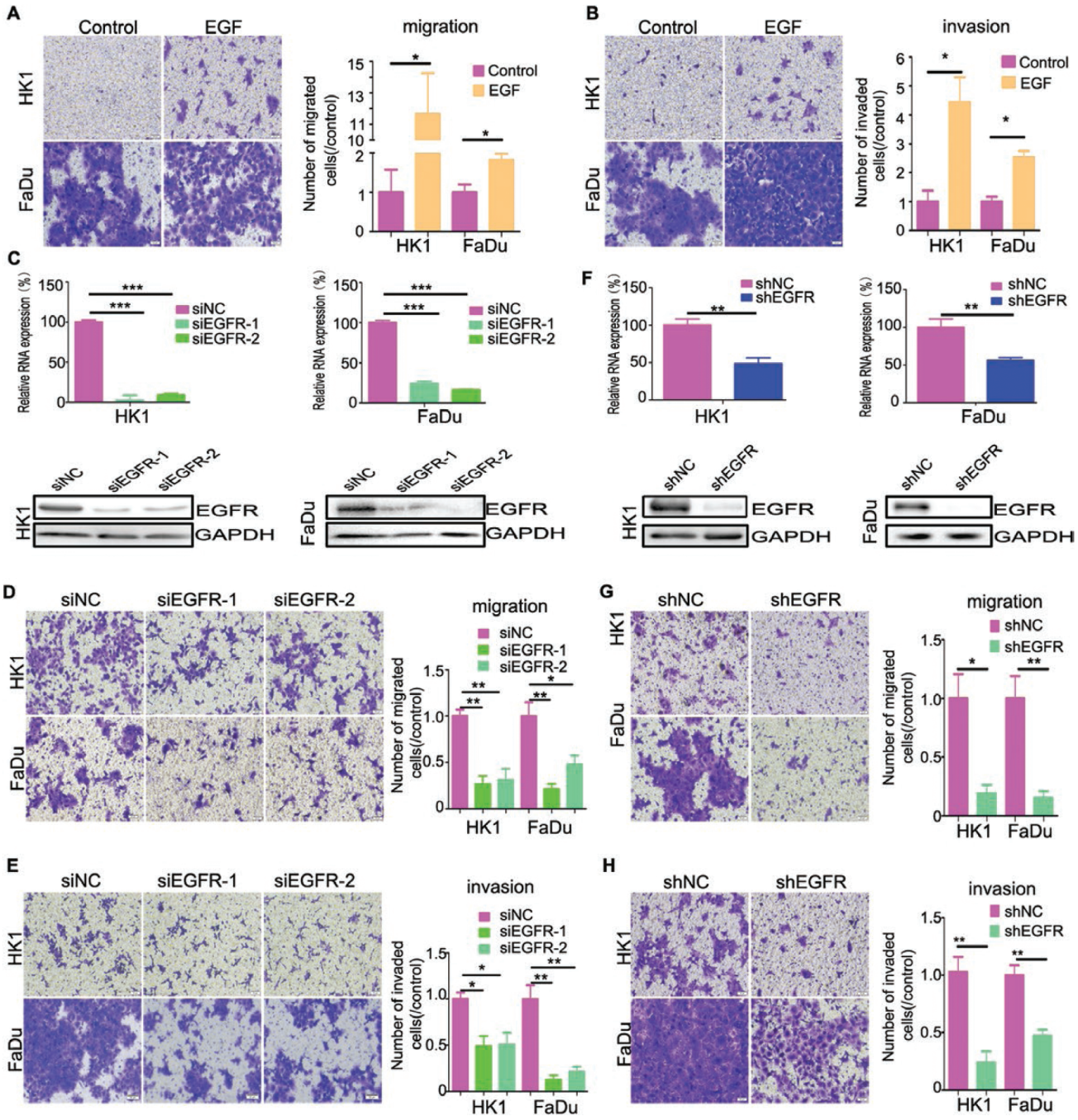


**Figure 2.** Activation of EGFR signaling promotes NPC cell migration and invasiveness *in vitro*. **(A,B)** Exogenous EGF (100 ng/ml) treatment stimulates migration (A) and invasiveness (B) of NPC cells. **(C)** EGFR was transiently silenced in NPC cells, and mRNA and protein levels of EGFR were measured by RT-PCR and western blot analysis, respectively. **(D,E)** Transient silencing of EGFR inhibits migration (D) and invasiveness (E) of NPC cells *in vitro*. **(F)** EGFR was stably silenced in NPC cells, and mRNA and protein levels of EGFR were measured by RT-PCR and western blot analysis, respectively. **(G, H)** Stable silencing of EGFR inhibits migration (G) and invasiveness (H) of NPC cells *in vitro*. * $P < 0.05$. ** $P < 0.01$. *** $P < 0.001$.

migration and invasion, the mRNA and protein levels of PKM2 in HK1 and FaDu cells were reduced by two separate siRNAs transfections (Supplementary Figure S2A, available at *Carcinogenesis* Online). Transient silencing of PKM2 in HK1 and FaDu cells resulted in a significant decrease in mobility and invasiveness *in vitro* (Supplementary Figure S2B and C, available at *Carcinogenesis* Online). Then, the mRNA and protein levels of PKM2 in HK1 and FaDu cells were stably inhibited by shRNA-expressing lentivirus (Supplementary Figure S2D, available at *Carcinogenesis* Online). Stable depletion of PKM2 dramatically attenuated tumor cell migration and invasion *in vitro* (Supplementary Figure S2E and F, available at *Carcinogenesis* Online), suggesting that the expression of PKM2 in NPC cells contributes to increased cell mobility and invasiveness. We then investigated whether PKM2 acts downstream of EGFR signaling in NPC cells. Western blot analysis revealed that silencing of EGFR by two siRNAs leads to decreased nuclear PKM2 protein levels in HK1 and FaDu cells (Figure 4A), whereas EGF treatment promotes

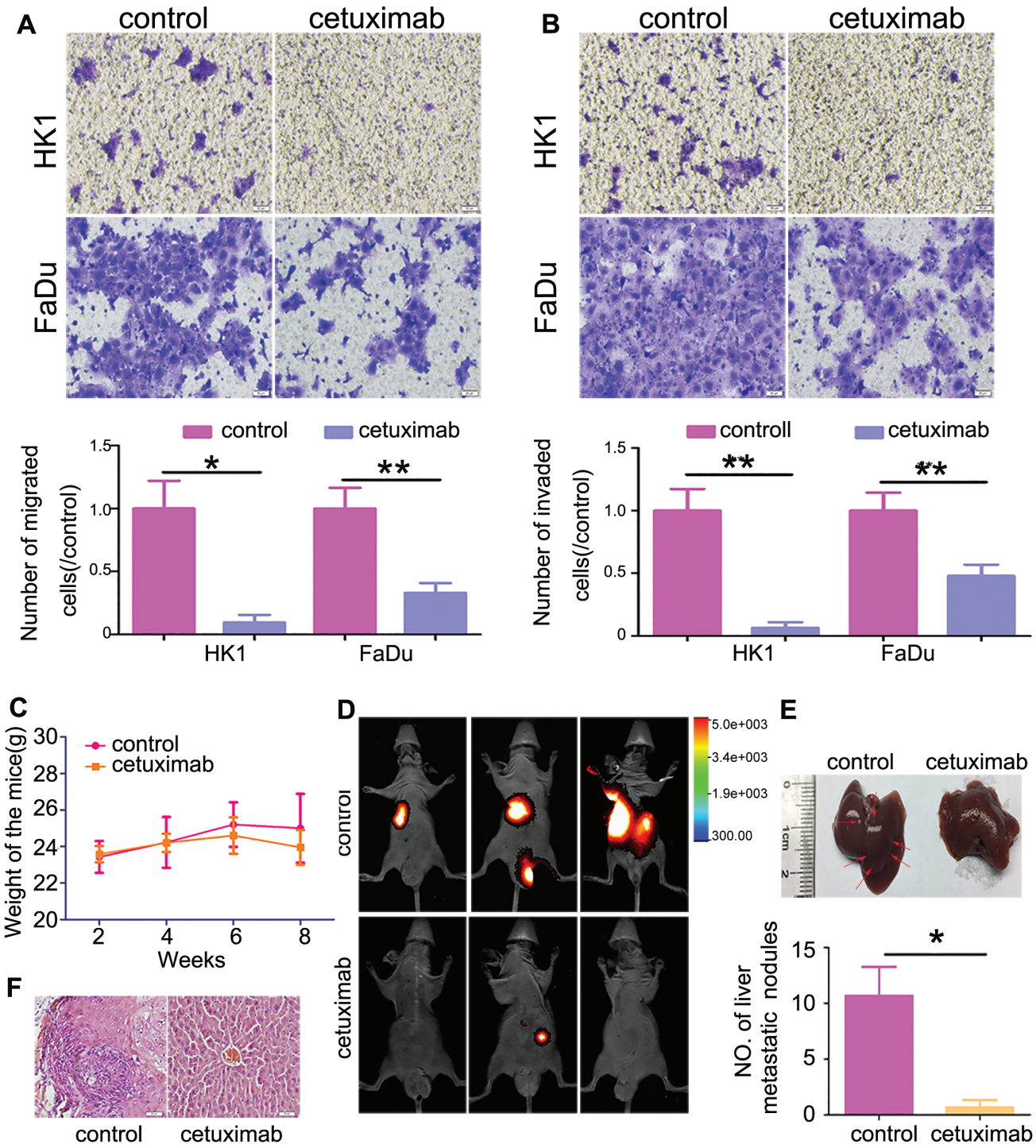


**Figure 3.** Blocking EGFR signaling by cetuximab suppresses NPC cell invasiveness *in vitro* and metastasis in vivo. **(A, B)** Cetuximab suppresses migration (A) and invasiveness (B) of NPC cells in vitro. **(C)** Luciferase-expressing HK1 cells were transplanted into the livers of nude mice and then the cetuximab-treated and untreated (control) mice were weighed. **(D)** Noninvasive bioluminescence imaging of luciferase-expressing intrahepatic HK1 xenografts showed that cetuximab suppresses orthotopic hepatic metastatic tumor formation. **(E)** A representative macroscopic image of control and cetuximab-treated nude mice. The tumor nodes were counted, and the data showed that cetuximab treatment reduced the number of liver tumor nodes. **(F)** H&E staining showed decreased metastatic tumor formation in the liver of cetuximab-treated mice. * $p < 0.05$. ** $p < 0.01$.

nuclear PKM2 expression (Figure 4B). We then demonstrated that EGF-stimulated NPC cell migration and invasiveness are dramatically suppressed by the loss of PKM2 (Figure 4C and D). Micheliolide (MCL) is a natural product that binds specifically to PKM2 and prevents its nuclear translocation (34). The western blot assay revealed that MCL treatment inhibited nuclear translocation of PKM2 protein in HK1 cells (Supplementary Figure S3, available at *Carcinogenesis* Online). More importantly, MCL treatment suppresses EGFR-stimulated NPC cell migration and invasiveness *in vitro* (Figure 4E and F), suggesting that nuclear

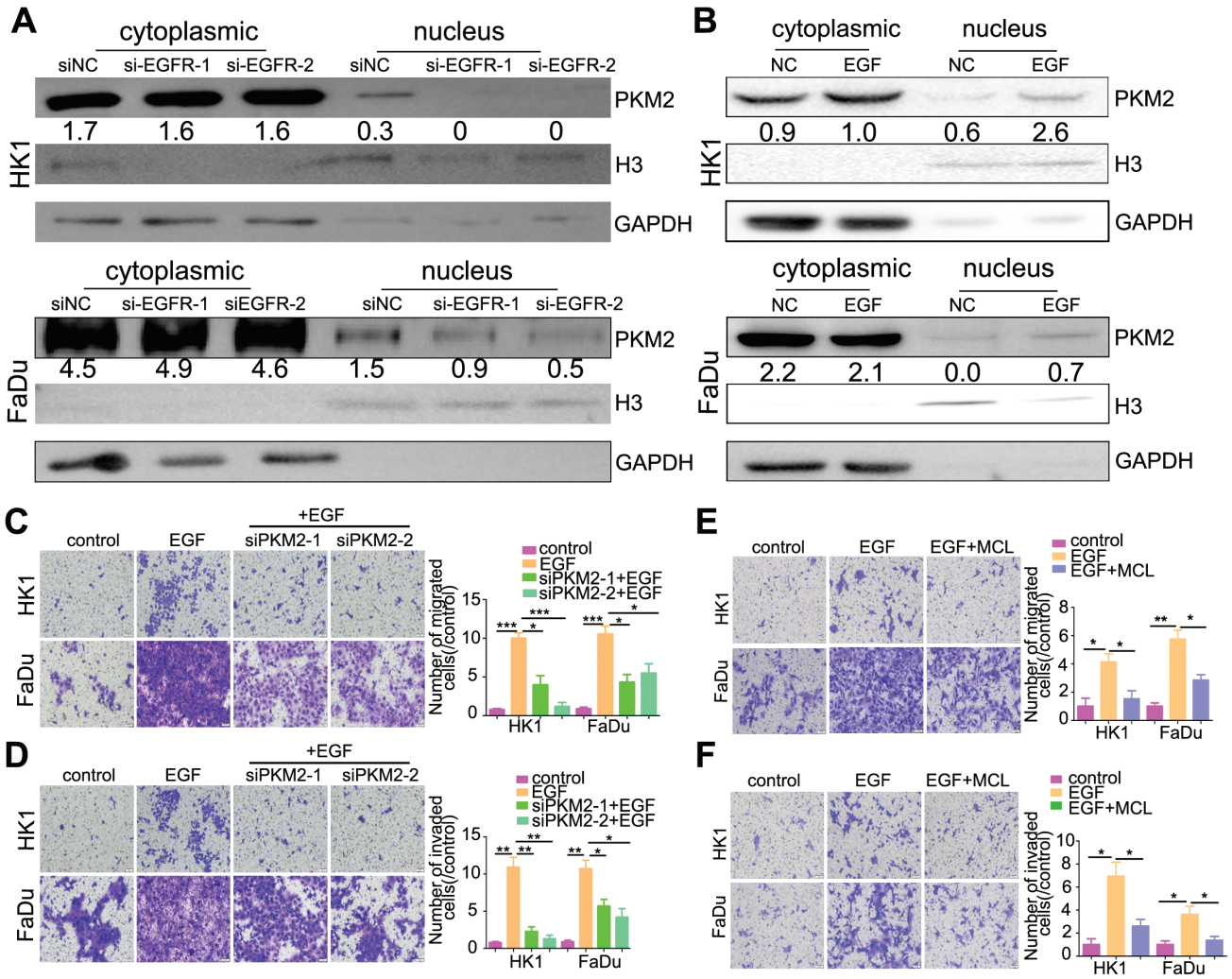


**Figure 4.** Activation of EGFR signaling promotes PKM2 nuclear translocation in NPC cells. **(A)** Transient silencing of EGFR leads to reduced nuclear PKM2 protein in HK1 and FaDu cells. The immune-intensity levels of cytoplasmic or nuclear PKM2 protein were normalized to GAPDH or histone 3 (H3), respectively. **(B)** Exogenous EGF treatment (100 ng/ml) promotes PKM2 nuclear translocation. **(C, D)** Depletion of PKM2 impairs EGF stimulated NPC cell migration (C) and invasion (D). **(E, F)** Inhibition of PKM2 nuclear translocation by micheliolide (MCL) treatment suppresses EGF-stimulated NPC cell migration (E) and invasion (F). * $p < 0.05$. ** $p < 0.01$. *** $p < 0.001$.

PKM2 contributes significantly to EGFR signaling-mediated NPC invasion. Furthermore, we demonstrated that high expression of nuclear PKM2 protein is associated with distant metastasis in NPC patients (Supplementary Table S4, available at *Carcinogenesis* Online); however, the association of total PKM2 protein level to distant metastasis was not significant (Supplementary Table S5, available at *Carcinogenesis* Online). Both total PKM2 and nuclear PKM2 protein level were associated with unfavorable OS and disease-free survival (DFS) in NPC patients (Supplementary Figure S4, available at *Carcinogenesis* Online).

## Depletion of either EGFR or PKM2 suppresses NPC cell metastasis *in vivo*

Next, we examined whether activation of EGFR-PKM2 signaling was required for tumor metastasis *in vivo*. A subhepatic transplantation model was employed to evaluate the metastatic potential of the EGFR- or PKM2-depleted HK1 cells. Either EGFR- or PKM2-depleted HK1 cells were orthotopically transplanted into the livers of nude mice. The weights of mice were recorded, and the data showed no difference between the three groups (Figure 5A and B). Eight weeks posttransplantation, the mice were sacrificed and liver tissues were obtained, fixed in 4% saline-buffered formalin, embedded in paraffin, sectioned at 5 μm, and stained with H&E. Morphological analysis (Figure 5C) and H&E staining (Figure 5D) confirmed that stable depletion of either EGFR or PKM2 effectively reduces liver metastatic tumor formation in the nude mice.

## Transcriptomic alterations induced by loss of EGFR-PKM2 signaling

We employed RNA-seq to search for the downstream effectors of EGFR-PKM2 signaling in NPC cells. A total of 648 genes are consistently upregulated, and 630 genes consistently downregulated, following loss of either EGFR or PKM2 expression in HK1 cells (Supplementary Figure S5A, available at *Carcinogenesis* Online). Among these downregulated genes, CCND1 was previously identified as a major target of EGFR-PKM2 signaling (22,33), indicating the robustness of our RNA profiling approach. Bioinformatics analysis (Supplementary Figure S5B and C, available at *Carcinogenesis* Online) revealed that the upregulated genes are mainly involved in the Hippo, Foxo, and melanogenesis signaling pathways regulating pluripotency. The

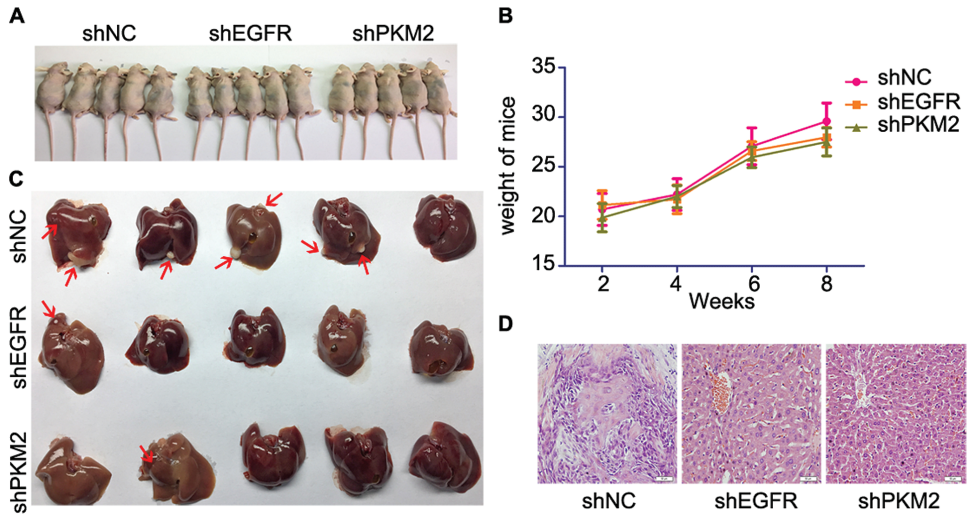


**Figure 5.** Stable silencing of either EGFR or PKM2 suppresses NPC cell metastasis *in vivo*. **(A)** A macroscopic image of nude mice transplanted with control cells, EGFR-depleted, or PKM2-depleted HK1 cells. **(B)** Body weights of mice transplanted with control cells, EGFR-depleted, or PKM2-depleted HK1 cells. **(C)** A macroscopic image of livers from nude mice transplanted with control cells, EGFR-depleted, or PKM2-depleted HK1 cells; arrows indicate metastatic tumor foci. **(D)** H&E staining shows metastatic NPC cells in the livers of mice transplanted with control cells and decreased metastatic tumor formation in the livers of mice transplanted with either EGFR-depleted or PKM2-depleted HK1 cells.

downregulated genes are associated with cytokine–cytokine receptor interaction, proteoglycans in cancer, MAPK signaling, Hippo signaling, and focal adhesion. GSEA (Supplementary Figure S5D, available at *Carcinogenesis* Online) further revealed that the downregulated genes are positively associated with Wnt/β-catenin signaling and epithelial–mesenchymal transition processes, which are involved in cancer metastasis (35–37). A number of differentially expressed genes were selected for further validation by RT-PCR (Supplementary Figure S5E, available at *Carcinogenesis* Online). For example, the mRNA levels of FOSL1, ANTXR2, CCND1, F3, EPHA2, and Vimentin are consistently decreased following EGFR or PKM2 depletion in HK1 and FaDu cells.

### FOSL1 and ANTXR2 contribute to EGF-stimulated NPC cell migration and invasion

Among those differentially expressed gene coregulated by EGFR and PKM2, FOSL1, and ANTXR2 are recently suspected to promote cancer progression (38,39). Western blot analysis showed that FOSL1 and ANTXR2 protein levels are downregulated in EGFR- or PKM2-silenced NPC cells (Figure 6A). To assess the biological function of FOSL1 and ANTXR2 in NPC invasion, either FOSL1 or ANTXR2 was inhibited by specific siRNAs. Depletion of either FOSL1 or ANTXR2 significantly suppresses EGF-stimulated NPC HK1 cell migration and invasion *in vitro* (Figure 6B), suggesting they are bonafide downstream effectors of EGF signaling-mediated NPC cell migration and invasion. Interestingly, both FOSL1 and ANTXR2 mRNAs levels are overexpressed in head and neck cancer samples according to the TCGA data. ChIP-qPCR assays revealed that PKM2 binds to the promoter regions of FOSL1 and ANTXR2, whereas loss of EGFR led to a decrease of PKM2 binding to those regions (Figure 6C). Similarly, silencing EGFR reduces PKM2 binding to the promoter of CCND1, which was previously identified as a target of the EGFR-PKM2 axis (33), confirming the robustness of our data. Transient silencing of PKM2 significantly attenuated EGF treatment induced FOSL1 and ANTXR2 mRNA levels in HK1 and FaDu cells (Figure 6D), indicating that nuclear PKM2 at least partially contributes to transactivation of FOSL1 and ANTXR2 upon EGFR activation.

By analyzing TCGA data, we demonstrated a positive association between the mRNA levels of either FOSL1 or ANTXR2 with EGFR or PKM2 in head and neck cancer samples (Figure 6E). We also measured these protein levels in a subset of NPC samples by immunohistochemical staining. The results clearly demonstrated that the protein levels of FOSL1 and ANTXR2 were positively correlated with EGFR and PKM2 (Supplementary Figure S6). More importantly, high expression of FOSL1 or ANTXR2 predicts an unfavorable prognosis in head and neck cancer patients (Figure 6F). Thus, our data strongly suggested that FOSL1 and ANTXR2 act as downstream effectors of EGFR-PKM2 signaling in NPC metastasis.

## Discussion

Distant metastasis occurs in approximately 20–30% of NPC patients (40). The prognosis of NPC patients with distant metastasis is very poor due to a lack of effective therapies (41). $^{18}$F-fluorodeoxyglucose (18F-FDG) positron emission tomography/computed tomography (PET/CT) is the most sensitive method for detecting distant metastasis of NPC, especially for bone metastasis. However, the efficacy of PET/CT in detecting liver metastasis is still suboptimal (42). For patients at high risk of metastasis, such as those with high nodal stage and nodal volume, assessment of the risk of distant metastasis before initial treatment of NPC is still a great challenge (43).

In this study, we found that intense EGFR immunostaining is associated with an increased risk of distant metastasis in NPC. We also provide evidence that blocking EGFR signaling efficiently suppressed NPC cell invasiveness *in vitro* and metastasis *in vivo*. Our data strongly suggest that EGFR is a promising biomarker for predicting the risk of distant metastasis. We envision the development of an EGFR immunostaining score model for assessing the risk of distant metastasis. For patients with extremely high levels of EGFR, in whom the metastasis cannot be imaged, more active systemic treatments or preventive treatments should be considered. A recent meta-analysis demonstrated that anti-EGFR monoclonal antibody treatment combined with radiotherapy or chemoradiotherapy significantly

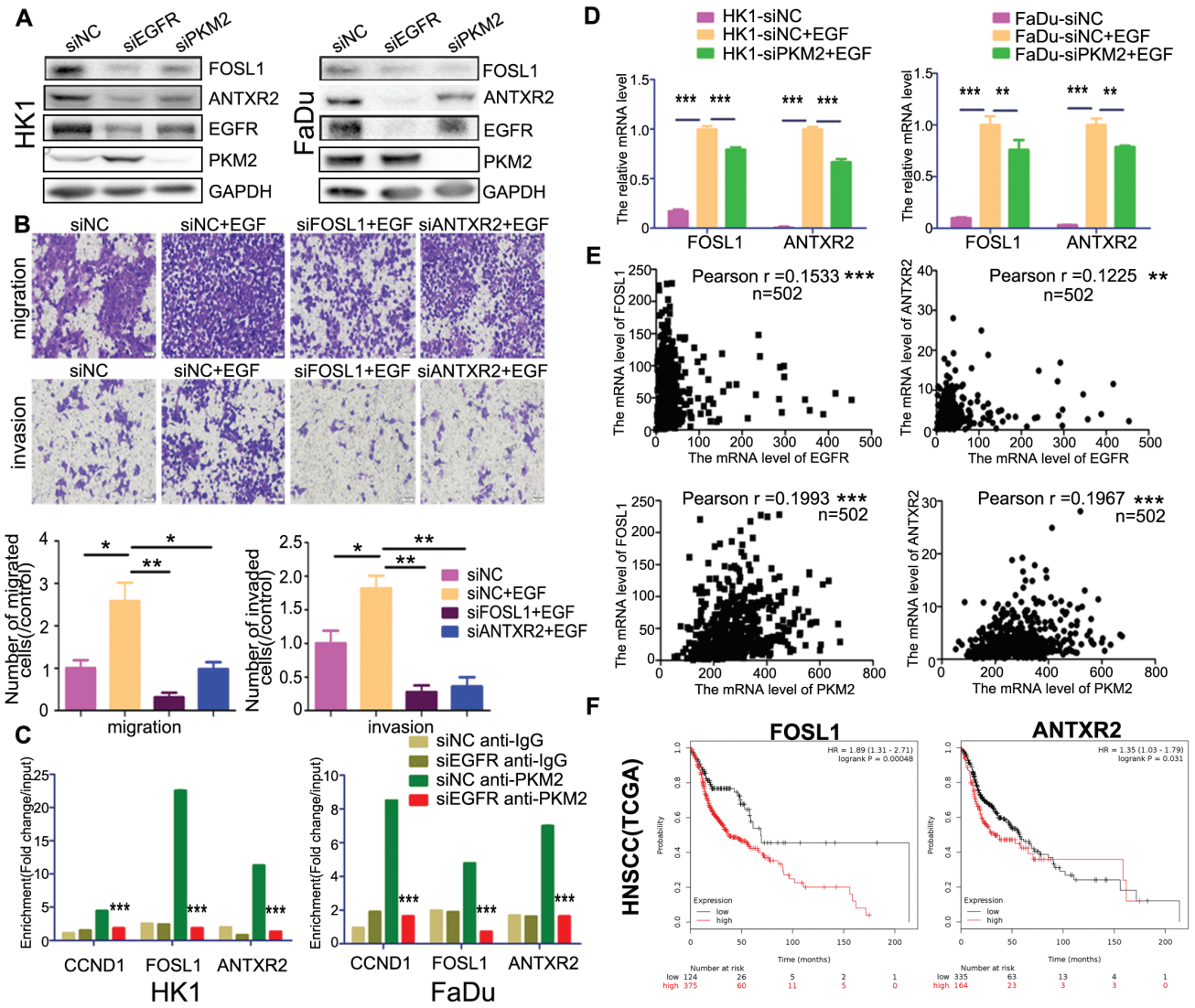


**Figure 6.** FOSL1 and ANTXR2 contribute to EGFR-PKM2 signaling-mediated tumor invasiveness. **(A)** Western blot analysis revealed a decrease in FOSL1 and ANTXR2 protein levels after silencing of EGFR and PKM2. **(B)** Silencing of either FOSL1 or ANTXR2 dramatically represses EGF-stimulated HK1 tumor cell migration and invasion. **(C)** Silencing of EGFR inhibited PKM2 binding to the promoter regions of FOSL1 and ANTXR2; CCND1 was used as a positive control. **(D)** Silencing PKM2 attenuated EGF-induced FOSL1 and ANTXR2 mRNA expression in HK1 and FaDu cells. **(E)** mRNA levels of FOSL1 and ANTXR2 are positively correlated with either EGFR or PKM2 mRNA levels. **(F)** High expression of FOSL1 or ANTXR2 predicts an unfavorable prognosis in head and neck cancer patients. * $p < 0.05$. ** $p < 0.01$. *** $p < 0.001$.

improved OS and DFS in NPC patients (44) with tolerable side effects. This suggests that locoregionally advanced NPC would likely benefit from anti-EGFR monoclonal antibody treatment. Our preclinical experiment showed that cetuximab effectively suppresses NPC cell metastasis in nude mice. Given that limited therapeutic options are available for NPC patients with distant metastasis after chemotherapy failure, our study supports the current treatment paradigm that blockage of EGFR signaling by anti-EGFR monoclonal antibodies is a feasible treatment for metastatic NPC.

Importantly, our preliminary studies demonstrate that nuclear PKM2 contributes significantly to increased mobility and invasiveness of NPC cells upon EGFR activation. Either total PKM2 or nuclear PKM2 protein level predicts unfavorable prognosis of NPC patients. We also provide evidence that MCL treatment inhibits NPC cell migration and invasion. MCL is a natural compound that binds with and selectively activates PKM2 (34). It has been shown that while PKM2 tetramers are distributed in the cytoplasm, PKM2 dimers are localized to the nucleus where they act as active protein kinases and regulate gene transcription and stimulate cancer cell proliferation (21). Covalent binding at cysteine residue 424 (C424) of PKM2 with MCL promotes its tetramer formation, thus inhibiting the translocation of PKM2 into the nucleus. An MCL derivate, dimethylaminomicheliolide, exerts growth-inhibitory effects on leukemia and glioma cells and is currently in clinical trial in Australia (34,45). We believe it is worth evaluating the antimetastatic potential of MCL in EGFR-overexpressing NPC cells.

By using a transcriptomic approach, a number of downstream target genes of EGFR and PKM2 were identified, and we selected FOSL1 and ANTXR2 for further functional validation. Silencing either FOSL1 or ANTXR2 suppressed EGF-stimulated NPC cell migration and invasion. It has been demonstrated that PKM2 regulates gene transcription through direct binding to the promoters of target genes, for example, MEK5 (21). The ability of PKM2 to regulate transcription is mainly dependent on

PKM2-mediated protein phosphorylation. Upon EGFR signaling activation, PKM2 binds to phosphorylated β-catenin, facilitating the recruitment of both proteins to the CCND1 promoter (22). Nuclear PKM2 phosphorylates histone H3 at T11 and promotes acetylation of histone H3 at lysine 9, leading to activation of CCND1 and c-myc transcription (33).

In this study, we observed that PKM2 binds to the promoter regions of FOSL1 and ANTXR2, and blocking EGFR signaling reduces PKM2 binding to these regions. Along with FOSL1 and ANTXR2, depletion of EGFR also reduces PKM2 binding to the CCND1 promoter. It is not clear which transcription factor cooperates with PKM2 in the process of EGF-induced FOSL1 and ANTXR2 expression. FOSL1 is a subunit of the AP-1 transcription factor complex. It was recently revealed that FOSL1 is required for KRAS-driven lung and pancreatic cancer. FOSL1 activates Aurora kinase A (AURKA) transcription, linking the KRAS oncogene to components of the mitotic machinery (46). FOSL1 also acts as an oncogene and transforms melanocytes through enhancement of several growth-promoting processes (47). Consistent with these observations, our findings suggest that FOSL1 is an attractive therapeutic target for various cancers, not only for controlling tumor growth but also for treatment of metastasis. ANTXR2 is also known as capillary morphogenesis protein 2 (CMG2) and participates in capillary morphogenesis. Overexpression of ANTXR2 is associated with poor prognosis of glioma patients. ANTXR2 promotes migration and invasion of glioma cells partially through enhancement of Yes-associated protein 1 (YAP1) activity (48). High expression of ANTXR2 is also associated with the invasion depth and lymph node metastasis of gastric cancer. Depletion of ANTXR2 in gastric cancer stem-like cells attenuates their self-renewing, invasive, and metastatic capabilities (39). In this study, we demonstrated that both FOSL1 and ANTXR2 are overexpressed in head and neck cancer, and their expression levels are positively correlated with either EGFR or PKM2 levels and predict unfavorable clinical outcomes of patients. The roles and underlying mechanisms of action of FOSL1 and ANTXR2 in NPC metastasis require further investigation.

In conclusion, we provide evidence that overexpression of EGFR is associated with distant metastasis in NPC. Upon EGFR signaling activation, PKM2 translocates to the nucleus and activates FOSL1 and ANTXR2 transcription, leading to increased migration and invasiveness in NPC. Our findings may contribute to the development of novel antimetastasis therapy for advanced NPC.

## Supplementary material

Supplementary data are available at *Carcinogenesis* online.

## Funding

This work was supported in part by grants from The National Natural Science Foundation of China (81572667, 81772902, 81872278, 81703131); the National "111" Project (Project #111–2–12); The Natural Science Foundation of Hunan Province, China (2018JJ1040); and Hunan Provincial Key Research and Development Program (2018SK2130, 2018SK2131).

*Conflict of interest statement:* None declared.

## References

1. Yi, M. *et al.* (2018) Rediscovery of NF-κB signaling in nasopharyngeal carcinoma: How genetic defects of NF-κB pathway interplay with EBV in driving oncogenesis? *J. Cell. Physiol.*, 233, 5537–5549.
2. Sham, J.S. *et al.* (1991) Role of bone scanning in detection of subclinical bone metastasis in nasopharyngeal carcinoma. *Clin. Nucl. Med.*, 16, 27–29.
3. Chua, M.L. *et al.* (2009) Comparison of 4 modalities for distant metastasis staging in endemic nasopharyngeal carcinoma. *Head Neck*, 31, 346–354.
4. Ng, S.H. *et al.* (2009) Pretreatment evaluation of distant-site status in patients with nasopharyngeal carcinoma: accuracy of whole-body MRI at 3-Tesla and FDG-PET-CT. *Eur. Radiol.*, 19, 2965–2976.
5. Tang, L.Q. *et al.* (2013) Prospective study of tailoring whole-body dual-modality [18F]fluorodeoxyglucose positron emission tomography/computed tomography with plasma Epstein–Barr virus DNA for detecting distant metastasis in endemic nasopharyngeal carcinoma at initial staging. *J. Clin. Oncol.*, 31, 2861–2869.
6. Liu, F.Y. *et al.* (2007) 18F-FDG PET can replace conventional work-up in primary M staging of nonkeratinizing nasopharyngeal carcinoma. *J. Nucl. Med.*, 48, 1614–1619.
7. Faivre, S. *et al.* (2004) Optimal management of nasopharyngeal carcinoma. *Curr. Opin. Oncol.*, 16, 231–235.
8. Li, J. *et al.* (2019) FOXA1 reprograms the TGF-β-stimulated transcriptional program from a metastasis promoter to a tumor suppressor in nasopharyngeal carcinoma. *Cancer Lett.*, 442, 1–14.
9. Wang, W. *et al.* (2018) Vimentin is a crucial target for anti-metastasis therapy of nasopharyngeal carcinoma. *Mol. Cell. Biochem.*, 438, 47–57.
10. Wang, W. *et al.* (2014) Oxidored-nitro domain containing protein 1 (NOR1) expression suppresses slug/vimentin but not snail in nasopharyngeal carcinoma: inhibition of EMT *in vitro* and *in vivo* in mice. *Cancer Lett.*, 348, 109–118.
11. Seshacharyulu, P. *et al.* (2012) Targeting the EGFR signaling pathway in cancer therapy. *Expert Opin. Ther. Targets*, 16, 15–31.
12. Lin, D.C. *et al.* (2014) The genomic landscape of nasopharyngeal carcinoma. *Nat. Genet.*, 46, 866–871.
13. Zheng, H. *et al.* (2016) Whole-exome sequencing identifies multiple loss-of-function mutations of NF-κB pathway regulators in nasopharyngeal carcinoma. *Proc. Natl. Acad. Sci. U. S. A.*, 113, 11283–11288.
14. Li, Y.Y. *et al.* (2017) Exome and genome sequencing of nasopharynx cancer identifies NF-κB pathway activating mutations. *Nat. Commun.*, 8, 14121.
15. Tu, C. *et al.* (2018) Identification of genomic alterations in nasopharyngeal carcinoma and nasopharyngeal carcinoma-derived Epstein-Barr virus by whole genome sequencing. *Carcinogenesis*. 39, 1517–1528.
16. Zheng, L.S. *et al.* (2017) SPINK6 promotes metastasis of nasopharyngeal carcinoma via binding and activation of epithelial growth factor receptor. *Cancer Res.*, 77, 579–589.
17. Shen, M. *et al.* (2019) Tinagl1 suppresses triple-negative breast cancer progression and metastasis by simultaneously inhibiting integrin/FAK and EGFR signaling. *Cancer Cell*, 35, 64–80.e7.
18. Yi, M. *et al.* (2019) 6-Phosphofructo-2-kinase/fructose-2,6-biphosphatase 3 and 4: a pair of valves for fine-tuning of glucose metabolism in human cancer. *Mol. Metab.*, 20, 1–13.
19. Yi, M. *et al.* (2018) Emerging role of lipid metabolism alterations in Cancer stem cells. *J. Exp. Clin. Cancer Res.*, 37, 118.
20. Christofk, H.R. *et al.* (2008) The M2 splice isoform of pyruvate kinase is important for cancer metabolism and tumour growth. *Nature*, 452, 230–233.
21. Gao, X. *et al.* (2012) Pyruvate kinase M2 regulates gene transcription by acting as a protein kinase. *Mol. Cell*, 45, 598–609.
22. Yang, W. *et al.* (2013) Nuclear PKM2 regulates the Warburg effect. *Cell Cycle*, 12, 3154–3158.
23. Cheng, T.Y. *et al.* (2018) Pyruvate kinase M2 promotes pancreatic ductal adenocarcinoma invasion and metastasis through phosphorylation and stabilization of PAK2 protein. *Oncogene*, 37, 1730–1742.
24. Chen, S. *et al.* (2018) Abberent expression of NOR1 protein in tumor associated macrophages contributes to the development of DEN-induced hepatocellular carcinoma. *J. Cell. Physiol.*, 233, 5002–5013.
25. Huang, D.P. *et al.* (1980) Establishment of a cell line (NPC/HK1) from a differentiated squamous carcinoma of the nasopharynx. *Int. J. Cancer*, 26, 127–132.
26. Hsu, C.M. *et al.* (2018) NVP-BEZ235, a dual PI3K-mTOR inhibitor, suppresses the growth of FaDu hypopharyngeal squamous cell carcinoma and has a synergistic effect with Cisplatin. *Cell Death Discov.*, 4, 57.

27. Anandharaj, A. *et al.* (2016) EBV and not HPV sensitizes tobacco-associated head and neck cancer cell line FaDu to radiotherapy. *Acta Otolaryngol.,* 136, 354–362.
28. Yi, M. *et al.* (2018) Dual-functionality of RASSF1A overexpression in A375 cells is mediated by activation of IL-6/STAT3 regulatory loop. *Mol. Biol. Rep.,* 45, 1277–1287.
29. Tarazona, S. *et al.* (2011) Differential expression in RNA-seq: a matter of depth. *Genome Res.,* 21, 2213–2223.
30. Yu, J. *et al.* (2007) Integrative genomics analysis reveals silencing of beta-adrenergic signaling by polycomb in prostate cancer. *Cancer Cell,* 12, 419–431.
31. Pierrefite-Carle, V. *et al.* (2002) Subcutaneous or intrahepatic injection of suicide gene modified tumour cells induces a systemic antitumour response in a metastatic model of colon carcinoma in rats. *Gut,* 50, 387–391.
32. García-Pérez, R. *et al.* (2018) Role of Kupffer cells in the progression of CRC liver metastases after the first stage of ALPPS. *Sci. Rep.,* 8, 8089.
33. Yang, W. *et al.* (2012) PKM2 phosphorylates histone H3 and promotes gene transcription and tumorigenesis. *Cell,* 150, 685–696.
34. Li, J. *et al.* (2018) Natural product micheliolide (MCL) irreversibly activates pyruvate kinase M2 and suppresses leukemia. *J. Med. Chem.,* 61, 4155–4164.
35. Brabletz, T. *et al.* (2018) EMT in cancer. *Nat. Rev. Cancer,* 18, 128–134.
36. Wang, W. *et al.* (2017) NOR1 suppresses cancer stem-like cells properties of tumor cells via the inhibition of the AKT-GSK-3β-Wnt/β-catenin-ALDH1A1 signal circuit. *J. Cell. Physiol.,* 232, 2829–2840.
37. Wang, W. *et al.* (2016) Significance of the NOR1-FOXA1/HDAC2-Slug regulatory network in epithelial-mesenchymal transition of tumor cells. *Oncotarget,* 7, 16745–16759.
38. Román, M. *et al.* (2019) Inhibitor of differentiation-1 sustains mutant KRAS-driven progression, maintenance, and metastasis of lung adenocarcinoma via regulation of a FOSL1 network. *Cancer Res.,* 79, 625–638.
39. Ji, C. *et al.* (2018) Capillary morphogenesis gene 2 maintains gastric cancer stem-like cell phenotype by activating a Wnt/β-catenin pathway. *Oncogene,* 37, 3953–3966.
40. Ai, Q.Y. *et al.* (2017) Prediction of distant metastases from nasopharyngeal carcinoma: improved diagnostic performance of MRI using nodal volume in N1 and N2 stage disease. *Oral Oncol.,* 69, 74–79.
41. Ai, Q.Y. *et al.* (2018) Nasopharyngeal carcinoma: relationship between invasion of the prevertebral space and distant metastases. *Eur. Arch. Otorhinolaryngol.,* 275, 497–505.
42. Xu, C. *et al.* (2017) Optimal modality for detecting distant metastasis in primary nasopharyngeal carcinoma during initial staging: a systemic review and meta-analysis of 1774 patients. *J. Cancer,* 8, 1238–1248.
43. Zhang, L., *et al.* (2019) Development and validation of a magnetic resonance imaging-based model for the prediction of distant metastasis before initial treatment of nasopharyngeal carcinoma: a retrospective cohort study. *EBioMedicine,* 40, 327–335.
44. Peng, L. *et al.* (2018) The efficacy and safety of anti-epidermal growth factor receptor monoclonal antibodies in nasopharyngeal carcinoma: literature-based meta-analyses. *J. Cancer,* 9, 4510–4520.
45. An, Y. *et al.* (2015) Micheliolide derivative DMAMCL inhibits glioma cell growth *in vitro* and *in vivo*. *PLoS One,* 10, e0116202.
46. Vallejo, A. *et al.* (2017) An integrative approach unveils FOSL1 as an oncogene vulnerability in KRAS-driven lung and pancreatic cancer. *Nat. Commun.,* 8, 14294.
47. Maurus, K. *et al.* (2017) The AP-1 transcription factor FOSL1 causes melanocyte reprogramming and transformation. *Oncogene,* 36, 5110–5121.
48. Tan, J. *et al.* (2018) Capillary morphogenesis protein 2 is a novel prognostic biomarker and plays oncogenic roles in glioma. *J. Pathol.,* 245, 160–171.